pain (1609; 2.39%), skin ulcers (non-diabetic) (1334; 1.98%), prurigo (1229; 1.82%), epidermal cysts (1194; 1.77%), vitiligo vulgaris (1134; 1.68%), seborrheic keratosis (1095; 1.62%) and drug eruption/toxicoderma (1018; 1.51%). These top 20 categories covered 57 577 (85.34%) of the 67 448 patients (Table 3).

## Age distributions of common diseases

The age distribution of atopic dermatitis was biphasic, peaking at 0–5 and 21–35 years of age (Fig. 1a). Tinea pedis peaked at 56–75 years of age (Fig. 1b). Tinea unguium showed a similar pattern (data not shown). Urticaria/angioedema showed a triphasic distribution pattern (Fig. 1c), whereas viral warts peaked at 6–15 years of age (Fig. 1d). Psoriasis peaked at 56–65 years of age (Fig. 2a). The age distribution for contact dermatitis was somewhat evenly dispersed

(Fig. 2b). The peak age for acne was 16–25 years (Fig. 2c), whereas that for seborrheic dermatitis was 71–75 (Fig. 2d). Hand eczema was distributed evenly in adults (Fig. 3a). The peak age for alopecia areata was 31–35 years (Fig. 3b). Herpes zoster/zoster-associated pain and prurigo were prominent in elderly patients (Fig. 3c,d). Epidermal cysts occurred in adults of all ages (Fig. 4a). Vitiligo vulgaris and drug eruption/toxicoderma were preponderant in elderly people (Fig. 4b,c). Notably, the age distribution for burns peaked in the group aged 0–5 years (Fig. 4d).

In Tables 4 and 5, we list the top five skin disorders for each age group. Miscellaneous eczema appeared in every age group, whereas atopic dermatitis was among the top five diseases for age groups under 50 years. The disease encountered most frequently in groups aged 6–40 years was atopic dermatitis.
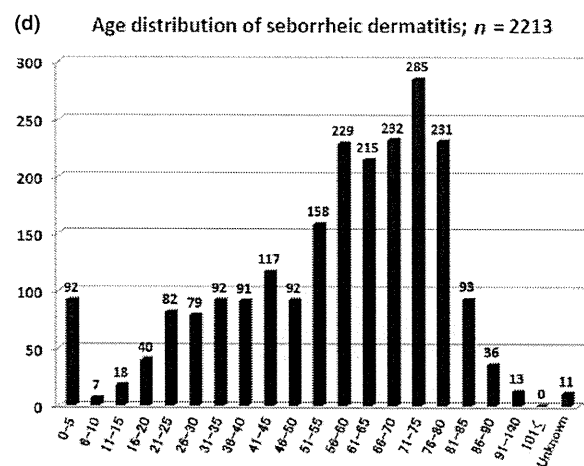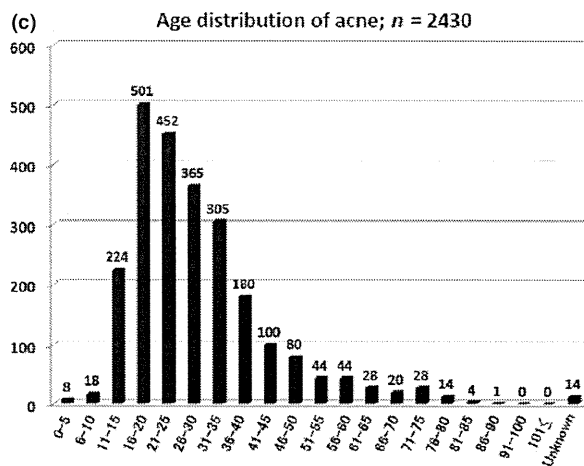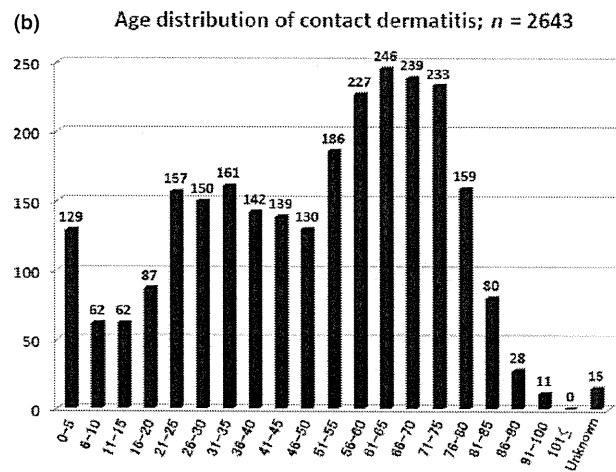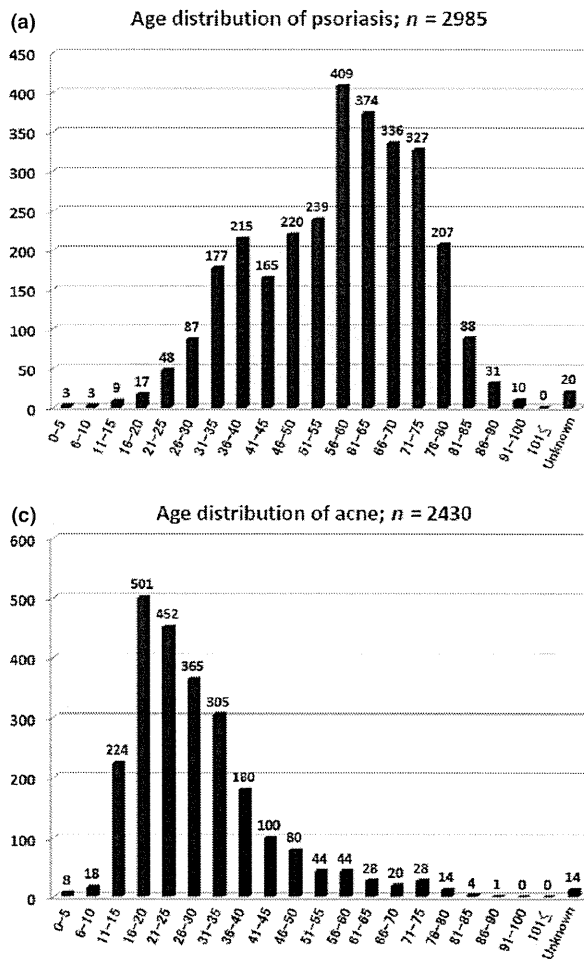


**Figure 2.** Age distribution of psoriasis, contact dermatitis, acne and seborrheic dermatitis.
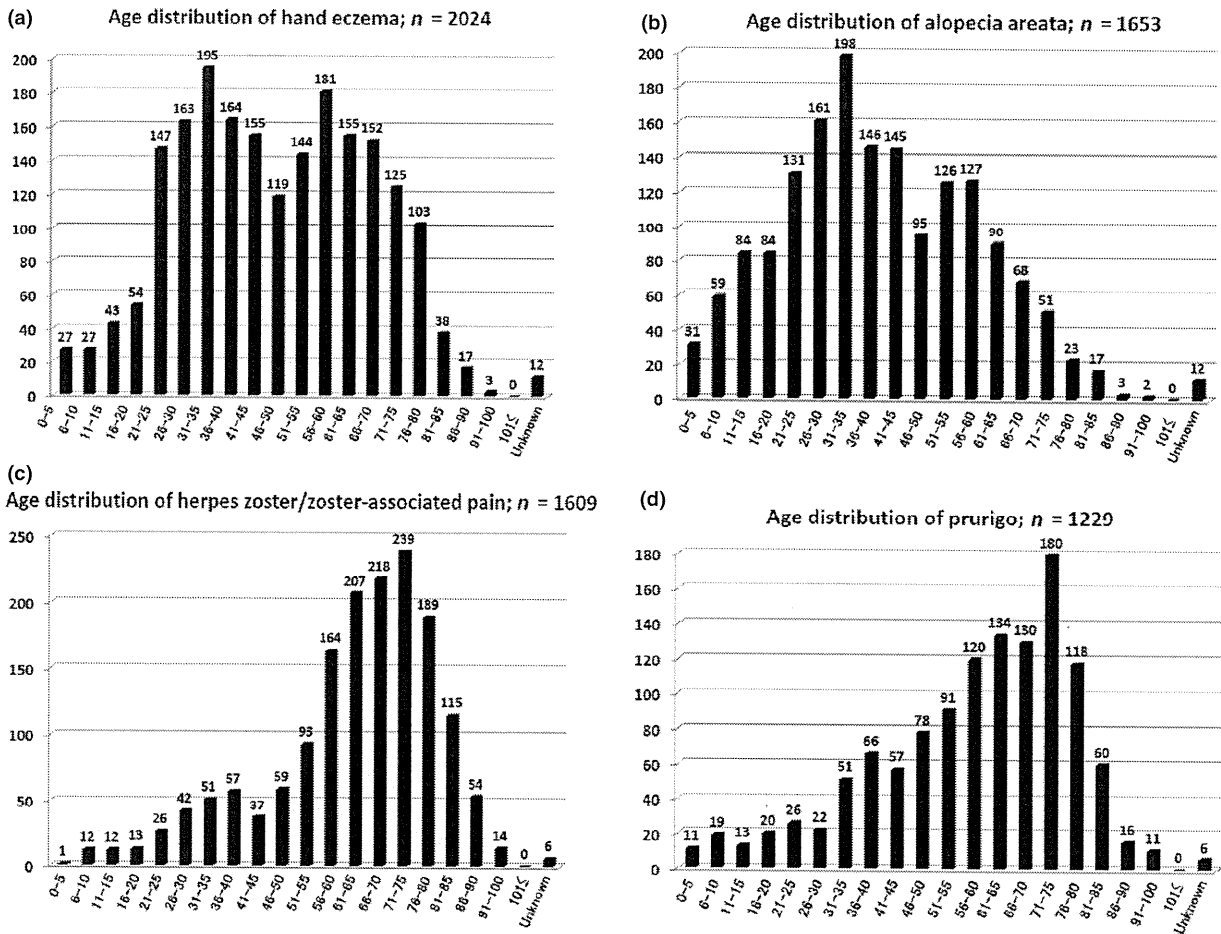
**Figure 3.** Age distribution of hand eczema, alopecia areata, herpes zoster/zoster-associated pain and prurigo.

Molluscum and impetigo were common in patients aged 0–10 years. Viral warts were among the top five diseases for groups aged 6–45 years. Acne was common in groups aged 11–35 years. Urticaria/angioedema was among the top five diseases for a wide range of age groups from 11–70 years old. Tinea pedis was common in groups aged above 41 years old. Psoriasis appeared in the top five diseases in middle-aged and older people with ages ranging 46–80 years old.

### Sex differences

Difference in the incidence of skin disorders between the sexes are shown in Table 6. The prevalence of diabetic dermatoses, psoriasis, androgenic alopecia, syphilis and erythroderma in males was more than twice that in females, whereas the prevalence of hand eczema, systemic sclerosis, systemic lupus erythematosus, dermatomyositis, reticular/racemous livedo, pigmented nevus, chloasma/senile freckle, erythema nodosum and rosacea/rosacea-like dermatitis was more than twice as high in females than males (Table 6).

### Correlation between patient numbers and the average low temperature, average high temperature and average humidity in the months of clinic visits

Because this study was a nationwide survey for Japan, a wide variation of climates had to be considered. We therefore searched for correlations between patient numbers and average low temperature, average high temperature and average humidity of the month in which patients visited clinics. The numbers of visiting patients diagnosed with urticaria/angioedema (Fig. 5), insect bites (Fig. 5), tinea pedis (Fig. 6)
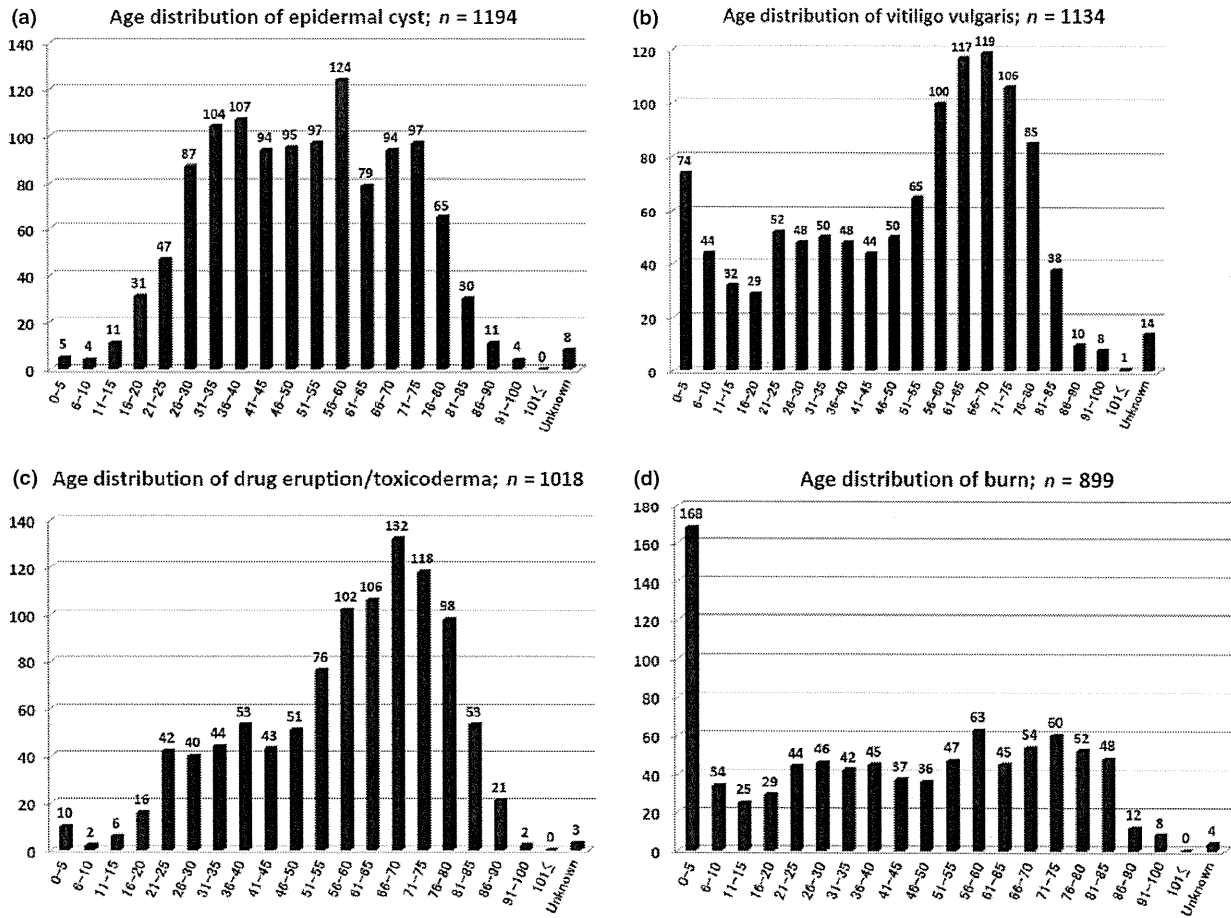
**Figure 4.** Age distribution of epidermal cyst, vitiligo vulgaris, drug eruption/toxicoderma and burn.

or impetigo (Fig. 6) showed a significant correlation with the average low temperature and with the average high temperature (data not shown). The numbers of visiting patients diagnosed with atopic dermatitis, contact dermatitis or molluscum contagiosum were also positively correlated with the average low temperature and average high temperature (data not shown). The numbers of patients diagnosed with seborrheic dermatitis showed a negative correlation with the average humidity (Fig. 7). The average humidity was also significantly and negatively correlated with atopic dermatitis, hand eczema and prurigo (data not shown).

## DISCUSSION

There are a number of limitations and biases in hospital-based prevalence studies, including institutional specificity (university hospital, pivotal local hospital or private clinic), differences in localization, climatic and seasonal differences, and differences in skills in diagnosis.[1,4–6] This study, conducted in fiscal year 2007 by the Japanese Dermatological Association, recruited 76 university hospitals, 55 district-based pivotal hospitals and 59 private clinics (190 clinics in total). We analyzed data for 67 448 patients that were collected seasonally from 170 clinics. This nationwide study is first of its kind in Japan, and its nature appears to eliminate, at least in part, some of the above-mentioned biases of hospital-based prevalence study.

In fiscal year 2007, eczematous and fungal diseases were commonly reported in dermatological clinics in Japan. The 20 most common categories of skin disorder were diagnosed in more than 85% of patients presenting dermatological complaints. A

**Table 4.** Top five skin disorders in each age group

| 0–5 years old (n = 4192) | | 26–30 years old (n = 3516) | |
|---|---|---|---|
| Miscellaneous eczema | 1229; 29.32% | Atopic dermatits | 826; 23.49% |
| Atopic dermatitis | 1078; 25.72% | Miscellaneous eczema | 451; 12.83% |
| Molluscum contagiosum | 425; 10.14% | Acne | 365; 10.38% |
| Impetigo contagiosum | 291; 6.94% | Urticaria/angioedema | 230; 6.54% |
| Miscellaneous benign skin tumors | 226; 5.39% | Viral wart | 215; 6.11% |
| **6–10 years old (n = 2099)** | | **31–35 years old (n = 4050)** | |
| Atopic dermatits | 505; 24.06% | Atopic dermatits | 824; 20.35% |
| Viral wart | 483; 23.01% | Miscellaneous eczema | 551; 13.6% |
| Miscellaneous eczema | 355; 16.91% | Acne | 305; 7.53% |
| Molluscum contagiosum | 144; 6.86% | Urticaria/angioedema | 251; 6.2% |
| Impetigo contagiosum | 110; 5.24% | Viral wart | 228; 5.63% |
| **11–15 years old (n = 1711)** | | **36–40 years old (n = 3807)** | |
| Atopic dermatits | 396; 23.14% | Atopic dermatits | 582; 15.29% |
| Viral wart | 294; 17.18% | Miscellaneous eczema | 503; 13.21% |
| Acne | 224; 13.09% | Urticaria/angioedema | 270; 7.09% |
| Miscellaneous eczema | 214; 12.51% | Psoriasis | 215; 5.65% |
| Urticaria/angioedema | 85; 4.97% | Viral wart | 203; 5.33% |
| **16–20 years old (n = 2270)** | | **41–45 years old (n = 3298)** | |
| Atopic dermatits | 624; 27.49% | Miscellaneous eczema | 454; 13.77% |
| Acne | 501; 22.07% | Atopic dermatits | 374; 11.34% |
| Miscellaneous eczema | 269; 11.85% | Urticaria/angioedema | 248; 7.52% |
| Viral wart | 150; 6.61% | Tinea pedis | 190; 5.76% |
| Urticaria/angioedema | 123; 5.42% | Viral wart | 175; 5.31% |
| **21–25 years old (n = 3219)** | | **46–50 years old (n = 3201)** | |
| Atopic dermatits | 843; 26.19% | Miscellaneous eczema | 453; 14.15% |
| Acne | 452; 14.04% | Tinea pedis | 236; 7.37% |
| Miscellaneous eczema | 407; 12.64% | Psoriasis | 220; 6.87% |
| Urticaria/angioedema | 206; 6.4% | Atopic dermatits | 215; 6.72% |
| Viral wart | 179; 5.56% | Urticaria/angioedema | 209; 6.53% |

**Table 5.** Top five skin disorders in each age group

| 51–55 years old (n = 4062) | | 76–80 years old (n = 4778) | |
|---|---|---|---|
| Miscellaneous eczema | 676; 16.64% | Miscellaneous eczema | 1304; 27.29% |
| Tinea pedis | 366; 9.01% | Tinea pedis | 463; 9.69% |
| Psoriasis | 239; 5.88% | Tinea unguium | 401; 8.39% |
| Urticaria/angioedema | 239; 5.88% | Seborrheic dermatitis | 231; 4.83% |
| Tinea unguium | 226; 5.56% | Psoriasis | 207; 4.33% |
| **56–60 years old (n = 5540)** | | **81–85 years old (n = 2636)** | |
| Miscellaneous eczema | 910; 16.43% | Miscellaneous eczema | 725; 27.5% |
| Tinea pedis | 534; 9.64% | Tinea unguium | 233; 8.84% |
| Psoriasis | 409; 7.38% | Tinea pedis | 230; 8.73% |
| Tinea unguium | 331; 5.97% | Herpes zoster/zoster-associated pain | 115; 4.36% |
| Urticaria/angioedema | 281; 5.07% | Seborrheic dermatitis | 93; 3.53% |
| **61–65 years old (n = 5415)** | | **86–90 years old (n = 1099)** | |
| Miscellaneous eczema | 1016; 18.76% | Miscellaneous eczema | 307; 27.93% |
| Tinea pedis | 519; 9.58% | Tinea unguium | 86; 7.83% |
| Tinea unguium | 393; 7.26% | Tinea pedis | 79; 7.19% |
| Psoriasis | 374; 6.91% | Pressure ulcer | 65; 5.91% |
| Urticaria/angioedema | 260; 4.8% | Skin ulcer (nondiabetic) | 63; 5.73% |
| **66–70 years old (n = 5628)** | | **91–100 years old (n = 427)** | |
| Miscellaneous eczema | 1141; 20.27% | Miscellaneous eczema | 110; 25.76% |
| Tinea pedis | 539; 9.58% | Pressure ulcer | 43; 10.07% |
| Tinea unguium | 463; 8.23% | Squamous cell carcinoma/Bowen's disease | 35; 8.2% |
| Psoriasis | 336; 5.97% | Skin ulcer (non-diabetic) | 28; 6.56% |
| Urticaria/angioedema | 250; 4.44% | Bullous pemphigoid | 22; 5.15% |
| **71–75 years old (n = 6157)** | | | |
| Miscellaneous eczema | 1457; 23.66% | | |
| Tinea pedis | 596; 9.68% | | |
| Tinea unguium | 566; 9.19% | | |
| Psoriasis | 327; 5.31% | | |
| Seborrheic dermatitis | 285; 4.63% | | |

**Table 6.** Sex differences in skin diseases

| | Total; Male; Female | | Total; Male; Female |
|---|---|---|---|
| Burn | 892, 1.33%; 414, 1.34%; 478, 1.32% | Miscellaneous viral disorders | 349, 0.52%; 171, 0.55%; 178, 0.49% |
| Trauma | 406, 0.61%; 196, 0.63%; 210, 0.58% | Syphilis | 24, 0.04%; 16, 0.05%; 8, 0.02% |
| Skin ulcer (nondiabetic) | 1318, 1.97%; 605, 1.96%; 713; 1.97% | Miscellaneous sexually transmitted | 40, 0.06%; 26, 0.08%, 14, 0.04% |
| Pressure ulcer | 606, 0.9%; 313, 1.01%; 293, 0.81% | diseases | |
| Miscellaneous physico-chemical | 675, 1.01%; 303, 0.98%; 372, 1.03% | Bullous pemphigid | 509, 0.76%; 208, 0.67%; 301, 0.83% |
| skin damage | | Pemphigus | 416, 0.62%; 180, 0.58%; 236, 0.65% |
| Diabetic dermatoses | 432, 0.64%; 300, 0.97%; 132, 0.37% | Miscellaneous bullous diseases | 139, 0.21%; 67, 0.22%; 72, 0.2% |
| Atopic dermatitis | 6707, 10.01%; 3486, 11.28%; 3221, 8.92% | Systemic sclerosis | 609, 0.91%; 94, 0.3%; 515, 1.43% |
| Hand eczema | 2009, 3%; 532, 1.72%; 1477, 4.09% | Systemic lupus erythematosus | 520, 0.78%; 72, 0.23%; 448, 1.24% |
| Contact dermatitis | 2629, 3.92%; 902, 2.92%; 1727, 4.78% | Dermatomyositis | 300, 0.45%; 76, 0.25%; 224, 0.62% |
| Seborrheic dermatitis | 2201, 3.28%; 1295, 4.19%; 906, 2.51% | Miscellaneous collagen diseases | 911, 1.36%; 209, 0.68%; 702, 1.94% |
| Miscellaneous eczema | 12523, 18.68%; 6289, 20.35%, 6234, 17.26% | Anaphylactoid purpura | 169, 0.25%; 72, 0.23%; 97, 0.27% |
| Urticaria/angioedema | 3355, 5.01%; 1251, 4.05%; 2104, 5.82% | Reticular/racemous livedo | 80, 0.12%; 21, 0.07%; 59, 0.16% |
| Prurigo | 1216, 1.81%; 755, 2.44%; 461, 1.28% | Miscellaneous vasculitis/purpura/ | 625, 0.93%; 239, 0.77%; 386, 1.07% |
| Drug eruption/toxicoderma | 1012, 1.51%; 436, 1.41%; 576, 1.59% | circulatory disturbance | |
| Psoriasis | 2967, 4.43%; 2138, 6.92%; 829, 2.29% | Mycosis fungoides | 418, 0.62%; 244, 0.79%; 174, 0.48% |
| Palmoplantar pustulosis | 828, 1.24%; 284, 0.92%; 544, 1.51% | Miscellaneous lymphomas | 283, 0.42%; 149, 0.48%; 134, 0.37% |
| Miscellaneous pustulosis | 170, 0.255%; 67, 0.22%; 103, 0.29% | Pigmented nevus | 703, 1.05%; 206, 0.67%; 497, 1.38% |
| Lichen planus | 200, 0.3%; 80, 0.26%; 120, 0.33% | Seborrheic keratosis | 1090, 1.63%; 537, 1.74%; 553, 1.53% |
| Miscellaneous inflammatory | 241, 0.36%; 95, 0.31%; 146, 0.4% | Soft fibroma/achrochordon | 228, 0.34%; 78, 0.25%; 150, 0.42% |
| keratotic disorders | | Epidermal cyst | 1183, 1.77%; 713, 2.31%; 470, 1.3% |
| Tylosis/clavus | 911, 1.36%; 292, 0.95%; 619, 1.71% | Lipoma | 171, 0.26%; 92, 0.3%; 79, 0.22% |
| Ichthyosis | 61, 0.09%, 31, 0.1%; 30, 0.08% | Dermatofibroma | 110, 0.16%; 44, 0.14%, 66, 0.18% |
| Miscellaneous keratinization | 502, 0.75%; 192, 0.62%; 310, 0.86% | Miscellaneous benign skin tumors | 1651, 2.46%; 673, 2.18%; 978, 2.71% |
| disorders | | Actinic keratosis | 256, 0.38%; 129, 0.42%; 127, 0.35% |
| Ingrown nail | 594, 0.89%; 197, 0.64%; 397, 1.1% | Basal cell carcinoma | 324, 0.48%; 166, 0.54%; 158, 0.44% |
| Miscellaneous nail disorder | 396, 0.59%; 123, 0.4%; 273, 0.76% | Squamous cell carcinoma/Bowen's | 447, 0.67%; 272, 0.88%; 175, 0.48% |
| Alopecia areata | 1644, 2.45%; 557, 1.8%; 1087, 3.01% | disease | |
| Androgenic alopecia | 208, 0.31%; 198, 0.64%; 10, 0.03% | Paget's disease | 221, 0.33%; 136, 0.44%; 85, 0.24% |
| Miscellaneous skin appendage | 266, 0.4%, 77, 0.25%; 189, 0.52% | Malignant melanoma | 802, 1.2%; 395, 1.28%; 407, 1.13% |
| disorders | | Miscellaneous malignant skin tumors | 531, 0.79%; 291, 0.94%; 240, 0.66% |
| Scabies | 96, 0.14%; 50, 0.16%; 46, 0.13% | Vitiligo vulgaris | 1123, 1.68%; 473, 1.53%; 650, 1.8% |
| Insect bite | 762, 1.14%; 285, 0.92%; 477, 1.32% | Chloasma/senile freckle | 334, 0.5%; 18, 0.06%; 316, 0.87% |
| Tinea pedis | 4363, 6.51%; 2225, 7.2%; 2138, 5.92% | Miscellaneous pigmented disorders | 154, 0.23%; 30, 0.1%; 124, 0.34% |
| Tinea unguium | 3216, 4.8%; 1581, 5.12%; 1635, 4.53% | Erythema multiforme | 194, 0.29%; 89, 0.29%; 105, 0.29% |
| Miscellaneous tinea | 607, 0.91%; 404, 1.31%; 203, 0.56% | Erythema nodosum | 111, 0.17%; 12, 0.04%; 99, 0.27% |
| Candidiasis | 406, 0.61%; 176, 0.57%; 230, 0.64% | Miscellaneous disorders with | 130, 0.19%; 40, 0.13%; 90, 0.25% |
| Miscellaneous mycosis | 209, 0.31%; 117, 0.38%; 92, 0.25% | erythematous plaques | |
| Acne | 2423, 3.62%; 757, 2.45%; 1666, 4.61% | Nevus/phacomatosis (other than | 266, 0.4%; 89, 0.29%; 177, 0.49% |
| Impetigo contagiosum | 505, 0.75%; 283, 0.92%; 222, 0.61% | pigmented nevus) | |
| Folliculitis | 749, 1.12%; 432, 1.4%; 317, 0.88% | Rosacea/rosacea-like dermatitis | 148, 0.22%; 36, 0.12%; 112, 0.31% |
| Erysipelas | 81, 0.12%; 35, 0.11%; 46, 0.13% | Granulomatous diseases | 192, 0.29%; 65, 0.21%; 127, 0.35% |
| Cellulitis | 589, 0.88%; 304, 0.98%; 285, 0.79% | Keloid/hypertrophic scar | 184, 0.27%; 73, 0.24%; 111, 0.31% |
| Miscellaneous bacterial infection | 909, 1.36%; 497, 1.61%; 412, 1.14% | Cheilitis/angular cheilitis/mucous | 94, 0.14%; 38, 0.12%; 56, 0.16% |
| Molluscum contagiosum | 602, 0.9%; 327, 1.06%; 275, 0.76% | membrane diseases | |
| Herpes simplex | 688, 1.03%; 266, 0.86%; 422, 1.17% | Erythroderma | 62, 0.09%; 44, 0.14%; 18, 0.05% |
| Herpes zoster/zoster-associated | 1599, 2.39%; 694, 2.25%; 905, 2.51% | Other diseases | 662, 0.99%; 315, 1.02%; 347, 0.96% |
| pain | | Total | 67 024, 100%; 30 899, 100%; |
| Viral wart | 3016, 4.5%; 1388, 4.49%; 1628, 4.51% | | 36 125, 100% |

## Urticaria/angioedema
### r = 0.155, P < 0.0001



Mean low temperature (°C)

## Insect bite
### r = 0.441, P < 0.0001



Mean low temperature (°C)

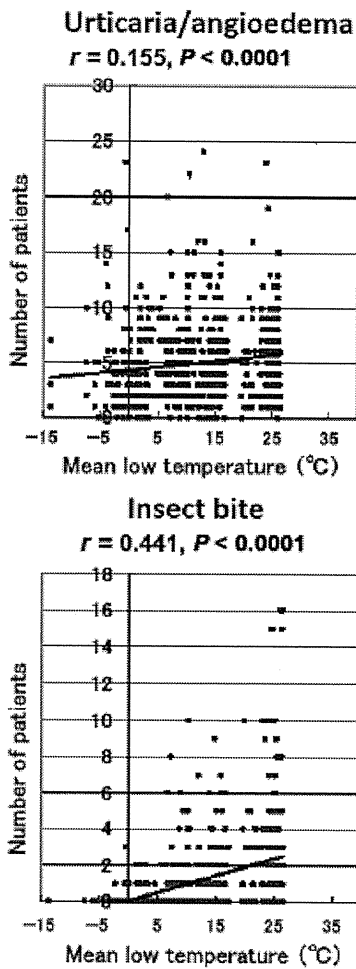**Figure 5.** Correlation between patient numbers and mean low temperature in urticaria/angioedema and insect bite.

## Tinea pedis
### r = 0.226, P < 0.0001



Mean low temperature (°C)

## Impetigo contagiosum
### r = 0.202, P < 0.0001
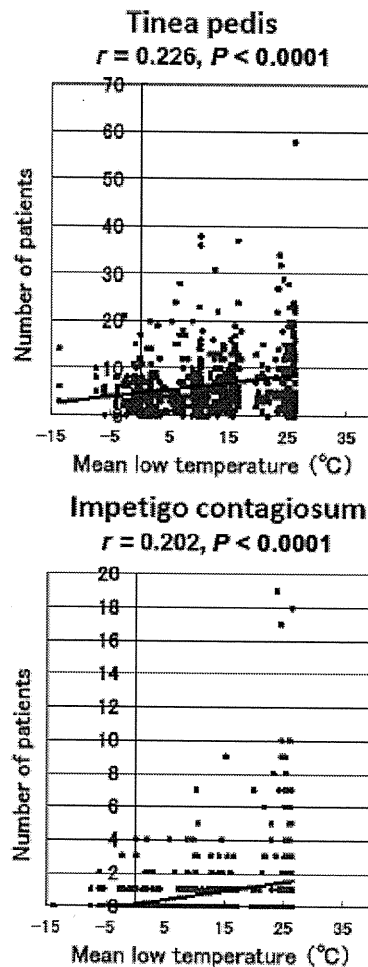


Mean low temperature (°C)

**Figure 6.** Correlation between patient numbers and mean low temperature in tinea pedis and impetigo contagiosum.

previous hospital-based study in Turkey[3] reported that the five most common disorders were atopic dermatitis, diaper dermatitis, impetigo, seborrheic dermatitis and miliaria in children aged 0–2 years; atopic dermatitis, impetigo, warts, contact dermatitis and insect bites in children aged 3–5 years; contact dermatitis, warts, atopic dermatitis, pruritus and impetigo in children aged 6–11 years; and acne, contact dermatitis, warts, seborrheic dermatitis and pruritus in children aged 12–16 years. For Dutch children aged 0–17 years old in 2001, the incidence rates per person-year of skin disorders were, in descending order, warts 34.3, dermatophytosis 25.4, contact dermatitis/other eczema 22.9, impetigo 20.5, laceration/cuts 20.3, atopic
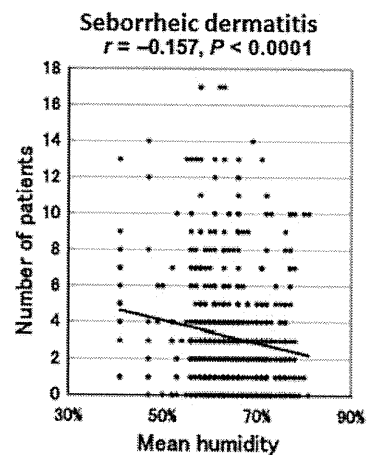
## Seborrheic dermatitis
### r = –0.157, P < 0.0001



Mean humidity

**Figure 7.** Negative correlation between patient numbers and mean humidity in seborrheic dermatitis.

dermatitis 16.5, moniliasis/candidasis 9.8 and molluscum contagiosum 9.5.[2] Although the order of each disease differed from country to country, atopic dermatitis, miscellaneous eczematous diseases, impetigo and warts appear to share their top rankings in pediatric dermatology, and this was also the case in Japan. Similar observations were also made in 1105 pediatric outpatients aged 0–15 years who visited the hospital of Aarau in Switzerland between 1998 and 2001.[7]

In Turkey, Yalçin *et al.*[8] examined records for 4099 geriatric patients over 65 years old who were admitted to the Ankara Numune Educational and Research Hospital from 1999 through 2003. The five most frequently diagnosed diseases were as follows: in the group aged 65–74 years, eczematous dermatitis, fungal infections, pruritus and bacterial and viral infections; in the group aged 75–84 years, eczematous dermatitis, pruritus, and fungal, viral and bacterial infections; and in the group aged over 85 years, pruritus, eczematous dermatitis, precancerous lesions and skin carcinomas, and viral and fungal infections.[8] In the present study, the Japanese geriatric population was also found to suffer very frequently from miscellaneous eczema and tinea pedis/unguium. In addition, there was a high incidence of psoriasis in elderly Japanese patients. As expected, we found conspicuous differences in the incidence of collagen diseases between the two sexes. A preponderance of collagen diseases in females was also evident in Yalçin's study.[8]

It should be emphasized again that this study was simply a measure of skin disorders in patients attending ordinary dermatology clinics in Japan. The study holds various limitations and biases, but it appears to highlight the current situation regarding patients presenting dermatological problems in Japan.

## ACKNOWLEDGMENTS

## REFERENCES

1 Julian CG. Dermatology in general practice. *Br J Dermatol* 1999; **141**: 518–520.
2 Mohammedamin RS, van der Wouden JC, Koning S *et al.* Increasing incidence of skin disorders in children? A comparison between 1987 and 2001 *BMC Dermatol* 2006; **6**: 4.
3 Tamer E, Ilhan MN, Polat M, Lenk N, Alli N. Prevalence of skin diseases among pediatric patients in Turkey. *J Dermatol* 2008; **35**: 413–418.
4 Steer AC, Jenney AW, Kado J *et al.* High burden of impetigo and scabies in a tropical country. *PLoS Negl Trop Dis* 2009; **3**: e467.
5 Elliot AJ, Cross KW, Smith GE, Burgess IF, Fleming DM. The association between impetigo, insect bites and air temperature: a retrospective 5-year study (1999–2003) using morbidity data collected from a sentinel general practice network database. *Fam Pract* 2006; **23**: 490–496.
6 Rørtveit S, Rortveit G. Impetigo in epidemic and non-epidemic phases: an incidence study over 4 (1/2) years in a general population. *Br J Dermatol* 2007; **157**: 100–105.
7 Wenk C, Itin PH. Epidemiology of pediatric dermatology and allergology in the region of Aargau, Switzerland. *Pediatr Dermatol* 2003; **20**: 482–487.
8 Yalçin B, Tamer E, Toy GG, Oztaş P, Hayran M, Alli N. The prevalence of skin diseases in the elderly: analysis of 4099 geriatric patients. *Int J Dermatol* 2006; **45**: 672–676.

# CASE LETTERS

## Extremely severe palmoplantar hyperkeratosis in a generalized epidermolytic hyperkeratosis patient with a keratin 1 gene mutation

*To the Editor:* Epidermolytic hyperkeratosis (EHK; OMIM#113800), also called bullous congenital ichthyosiform erythroderma, is a rare genetic disorder of keratinization. We report a patient with generalized EHK showing extremely severe palmoplantar hyperkeratosis with digital contractures.

A 45-year-old Japanese man had erythroderma at birth. He exhibited skin blistering, erosions, and hyperkeratosis on the erythrodermic skin since infancy. The blistering and erosions gradually diminished with age. He developed severe palmoplantar hyperkeratosis and digital contractures at 7 years of age. At 24 years of age, surgery was performed to improve the contraction of his toes. A physical examination revealed hyperkeratosis of the entire body, especially at the ankles, elbows, and knees, and erosions were observed on the inner side of the elbows and knees (Fig 1, *A-D*). Palmoplantar hyperkeratosis was severe with digital contractures. The

morphology of his hair, nails, and teeth was normal. There was no known family history of skin disease. Skin biopsy from the upper portion of the left arm showed severe granular degeneration in all the suprabasal layers (Fig 1, *E*). Ultrastructural analysis revealed clumping of the intermediate filaments within keratinocytes of the suprabasal layers (Fig 1, *F*).

Direct sequencing of the whole coding regions of *KRT1* and *KRT10* (GenBank accession numbers NT029419.11 and NT010755.15) was performed as previously described,[1] and a novel heterozygous *KRT1* missense mutation c.1457T>G ( p.Leu486Arg) was identified in exon 7. This mutation was verified by restriction enzyme *Msp*I digestion. The mutation p.Leu486Arg was not found in 100 normal, unrelated Japanese alleles (50 healthy unrelated individuals) using sequence analysis (data not shown).

The present novel *KRT1* mutation p.Leu486Arg is in the 2B segment of keratin 1 (Fig 2, *A* and *B*). This mutation occurred within the highly conserved helix termination motif (HTM) of the K1 protein. The palmoplantar hyperkeratosis was extremely severe. It is noteworthy that another mutation at the identical
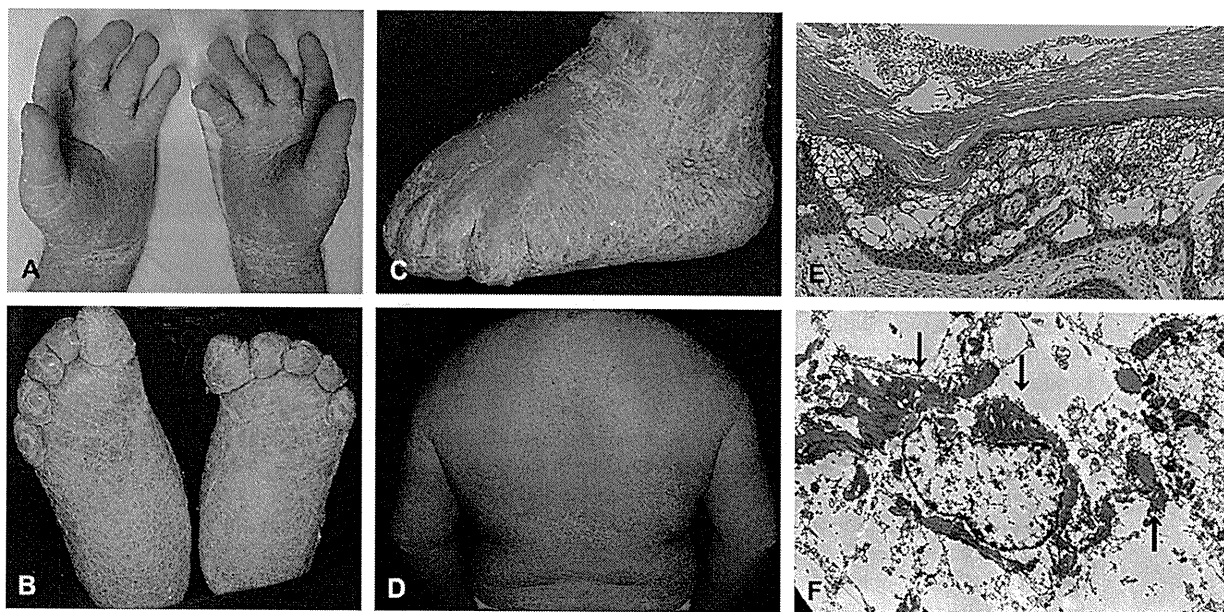


**Fig 1.** Clinical, histopathologic, and ultrastructural features of the patient. Severe diffuse hyperkeratosis and scale are seen on the palms (**A**) and soles (**B**). Warty brown hyperkeratosis and scale are present on the margins and the dorsal surface of the foot (**C**). Generalized erythroderma and scaling is seen on the trunk (**D**). The histopathologic examination revealed acanthosis and hyperkeratosis, coarse keratohyaline granules, and severe granular degeneration in the entire spinous and granular layers of the epidermis (**E**). Ultrastructurally, clumping of the keratin filaments *(arrows)* is seen within an upper epidermal keratinocyte (**F**).

**Keratin 1**

**A**



**Heptad repeats in HIM and HTM**

**B**

```
Position →a  d    a  d    a  d    a  d    a        d   a  d   a  d
Amino acid sequence→ IKSLNNQFASFIDKVRFLEQQNQVLQTKWEL      LALDLEIATYRTLLEGEESR
Mutation→  ↑↑↑  ↑↑         ↑      ↑      ↑↑↑↑  ↑  ↑↑
           ①②③  ④⑤         ⑥      ⑦      ⑧⑨⑩⑪  ⑫  ⑬⑭
```

**C**

| | Mutation | Hydropathy index | Pamloplantar hyperkeratosis |
|---|---|---|---|
| ① | S186P | -0.8→ -1.6 | ND |
| ② | L187F | 3.8→ 2.8 | mild |
| ② | L187F | 3.8→ 2.8 | mild |
| ③ | N188S | -3.5→ -0.8 | ND |
| ③ | N188S | -3.5→ -0.8 | severe |
| ③ | N188S | -3.5→ -0.8 | severe |
| ③ | N188K | -3.5→ -3.9 | severe |
| ③ | N188T | -3.5→ -0.7 | ND |
| ④ | F191I | 2.8→ 4.5 | mild |
| ④ | F191C | 2.8→ 2.5 | severe |
| ⑤ | S193P | -0.8→ -1.6 | severe |
| ⑥ | L208P | 3.8→ -1.6 | severe |
| ⑦ | L214P | 3.8→ -1.6 | mild |
| ⑧ | E478K | -3.5→ -3.9 | mild |
| ⑧ | E478D | -3.5→-3.5 | mild |
| ⑨ | I479F | 4.5→2.8 | mild |
| ⑨ | I479F | 4.5→ 2.8 | mild |
| ⑨ | I479T | 4.5→ -0.7 | mild |
| ⑨ | I479T | 4.5→ -0.7 | mild |
| ⑩ | T481P | -0.7→ -1.6 | severe |
| ⑪ | Y482C | -1.3→ 2.5 | mild |
| ⑫ | L486P | 3.8→ -1.6 | severe |
| ⑫ | L486R | 3.8→ -4.5 | severe |
| ⑬ | E489K | -3.5→ -3.9 | mild |
| ⑭ | E490Q | -3.5→ -3.5 | mild |
| ⑭ | E490G | -3.5→ -0.4 | mild |

ND, not described.
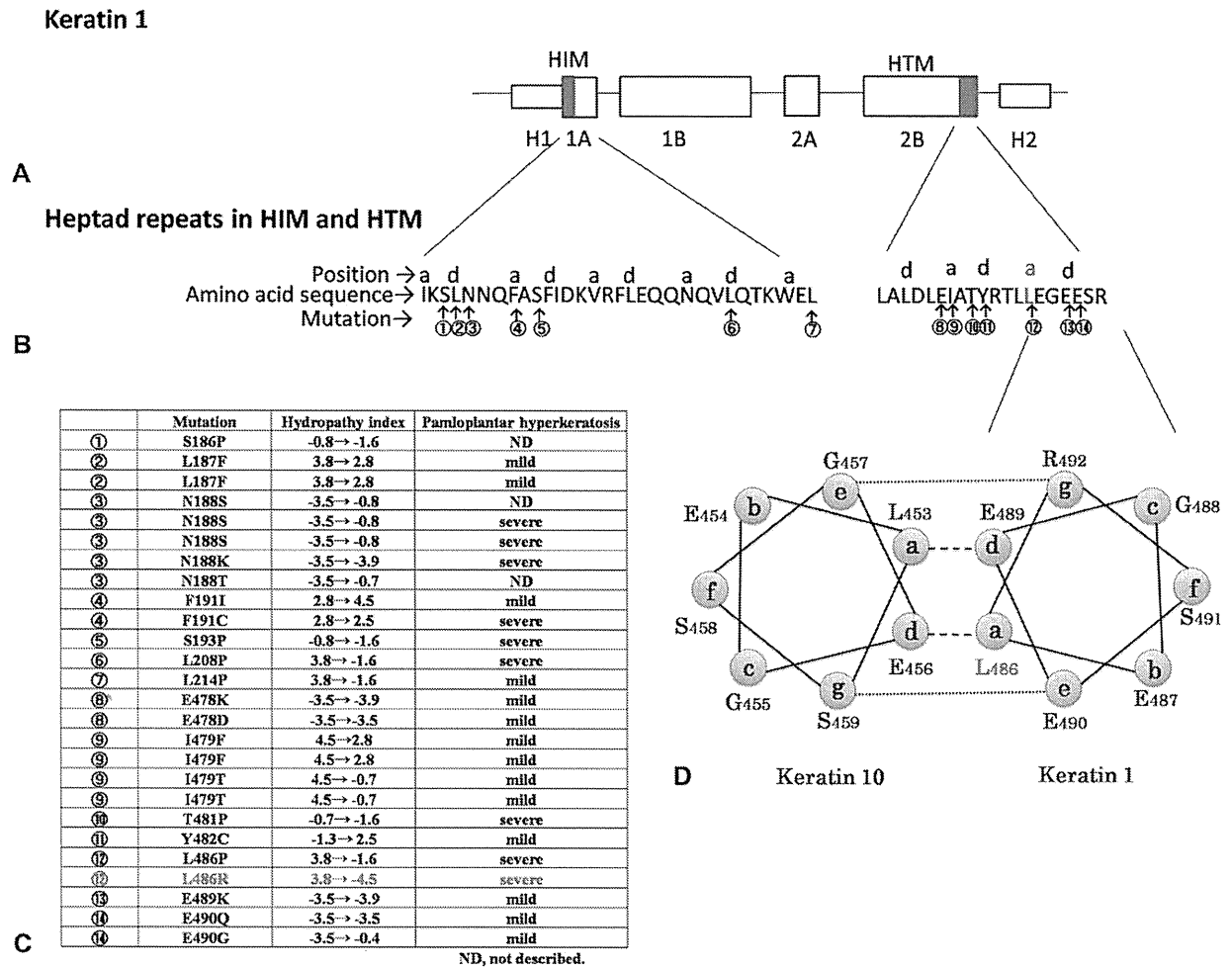
**D**



Keratin 10          Keratin 1

**Fig 2.** Summary of mutations in the helix initiation motif (HIM) and helix termination motif (HTM) of K1 from the Human Intermediate Filament Database (www.interfil.org/). **A**, Molecular structure of K1. **B**, Heptad repeats in HIM and HTM of K1 and mutation sites. The majority of cases (22 of 26) had mutations in the heptad repeat position *a, d, e,* and *g.* The present mutation is located at the *a* position leucine residue at codon no.486 *(red characters)* in the C-terminal—most heptad repeat. **C**, Summary of the *KRT1* mutations in HIM and HTM, alterations of hydropathy index, and levels of palmoplantar hyperkeratosis. Eight cases, including the present one, were reported as showing severe palmoplantar hyperkeratosis, and seven of those nine patients harbored mutations in the important *a, d, e,* and *g* position of heptad repeats. Mutations in this 486-leucine residue may seriously perturb the stability of keratin intermediate filaments. The substitution of arginine for leucine alters the character of the amino acid from that of a hydrophobic, apolar amino acid (hydropathy index of leucine, +3.8) to that of the most hydrophilic, basic amino acid (hydropathy index of arginine, −4.5). **D**, Heptad structure of the rod domain: schematic of a transverse cut through the last heptad *(abcdefg)* of the HTM of K1 and K10, showing hydrophobic interactions between positions *a* and *d (dashed lines)* and ionic hydrogen interactions between positions *e* and *g (dotted lines).* Position *a* is occupied by apolar, hydrophobic amino acids. The *a* residues are thought to interact with amino acids located in the *d* position of the partner molecule of the heterodimer through hydrophobic interactions which stabilize the two-chain coiled-coil molecules. When the two strands coil around each other, positions *a* and *d* are internalized, stabilizing the structure, while positions *b, c, e, f,* and *g* are exposed on the surface of the protein. Residues at positions *e* and *g* stabilize dimer formation through ionic and hydrogen bonds.

position of K1, p.Leu486Pro, was reported in patients with EHK and severe palmoplantar hyperkeratosis (Fig 2, *C*) and digital contractures, and the affected individuals exhibited clinical features similar to our patient.[2] Therefore, our data suggest that a nonconservative amino acid change at codon 486 of K1 results in a severe form of generalized EHK.

The rod domains consist of four alfa-helical segments that possess a repeating heptad amino acid residue peptide motif *(a-b-c-d-e-f-g)n* that has the potential to form a two-chain coiled coil with a corresponding sequence (Fig 2, *D*).[3-5] The residues at position *a, d, e,* and *g* are considered to be highly sensitive to mutations.[6]

Our patient with generalized EHK had most severe palmoplantar hyperkeratosis compared to previously reported cases with mutations in *KRT1*. The leucine residue at codon 486 is located in the *a* position of the heptad repeat at the C-terminal end of the 2B helix, and the substitution of arginine for leucine seriously alters the character of amino acid. It is therefore reasonable to say that this mutation caused generalized EHK with severe palmoplantar hyperkeratosis, compared with that seen in patients harbouring mutations in the other residues.

Twenty-six EHK cases, including the present case with point mutations at the helix initiation motif (HIM) and HTM of *KRT1*, have been reported to date (Fig 2, *C*); Human Intermediate Filament Database [www.interfil.org/]). Only nine cases, including the present case, were diagnosed as generalized EHK with severe palmoplantar hyperkeratosis, and seven cases out of nine harbored missense mutations in the heptad repeat position *a, d, e,* and *g*. These facts indicate that the mutation site and the nature of amino acid alterations in K1 may determine the level of severity of palmoplantar hyperkeratosis.

*Rinko Osawa, MD,[a] Masashi Akiyama, MD, PhD,[a] Kentaro Izumi, MD,[a] Hideyuki Ujiie, MD,[a] Kaori Sakai, MS,[a] Ikue Nemoto-Hasebe, MD,[a] Teruki Yanagi, MD,[a] Hiroko Koizumi, MD, PhD,[b] and Hiroshi Shimizu, MD, PhD[a]*

*Department of Dermatology,[a] Hokkaido University Graduate School of Medicine, Sapporo, Japan, and the Koizumi Dermatology Clinic,[b] Sapporo, Japan*

*Correspondence to: Rinko Osawa, MD, Department of Dermatology, Hokkaido University Graduate School of Medicine, N15 W7, Kita-ku, Sapporo 060-8638, Japan*

*E-mail: r-osawa@fm2.seikyou.ne.jp*

**REFERENCES**
1. Tsubota A, Akiyama M, Sakai K, Goto M, Nomura Y, Ando S, et al. Keratin 1 gene mutation detected in epidermal nevus with epidermolytic hyperkeratosis. J Invest Dermatol 2007;127:1371-4.
2. Lee DY, Ahn KS, Lee CH, Rho NK, Lee JH, Lee ES, et al. Two novel mutations in the keratin 1 gene in epidermolytic hyperkeratosis. J Invest Dermatol 2002;119:976-7.
3. Müller FB, Küster W, Wodecki K, Almeida H Jr, Bruckner-Tuderman L, Krieg T, et al. Novel and recurrent mutations in keratin KRT5 and KRT14 genes in epidermolysis bullosa simplex: implications for disease phenotype and keratin filament assembly. Hum Mutat 2006;27:719-20.
4. Lu Y, Guo C, Liu Q, Zhang X, Cheng L, Li J, et al. A novel mutation of keratin 9 in epidermolytic palmoplantar keratoderma combined with knuckle pads. Am J Med Genet A 2003;120:345-9.
5. Coulombe PA, Fuch E. Elucidating the early stages of keratin filament assembly. J Cell Biol 1990;111:153-69.
6. Heald R, McKeon F. Mutations of phosphorylation sites in lamin A that prevent nuclear lamina disassembly in mitosis. Cell 1990;61:579-89.

## Scrotal elephantiasis secondary to hidradenitis suppurativa

*To the Editor:* We read with great interest the continuing medical education article by Alikhan et al[1] in the April 2009 issue of the *Journal* providing a comprehensive review of hidradenitis suppurativa (HS). We found the mention of scrotal lymphedema caused by HS to be of particular interest and would like to share our experience with a patient who developed the unusual complication of scrotal elephantiasis caused by longstanding HS.

A 58-year-old white man with no recent travel history who lived in social isolation presented with scrotal enlargement that began about a decade ago but had become notably worse over the past 3 years. He denied any history of sexually transmitted infections and recalled having had HS his entire adult life. The patient underwent several incision and drainage procedures in the emergency department over the years, had recently been treated briefly with oral antibiotics without improvement, and was finally referred for dermatologic evaluation. The physical examination revealed a massively enlarged, indurated scrotum that obscured his penis and had multiple sinus tracts draining clear, foul-smelling fluid (Fig 1). He had many violaceous nodules with open comedones in the intertriginous regions, including the left and right axillae, bilateral groins, bilateral inner thighs, and beneath the skin folds on his lower abdomen.

Punch biopsy specimens from the patient's left inner thigh and left lower abdomen revealed findings

*Case Report*

# A Case of Cystic Basal Cell Carcinoma Which Shows a Homogenous Blue/Black Area under Dermatoscopy

**Akihiro Yoneta,[1] Kohei Horimoto,[1] Keiko Nakahashi,[1] Satoru Mori,[1] Kazuo Maeda,[2] and Toshiharu Yamashita[1]**

[1] *Department of Dermatology, School of Medicine, Sapporo Medical University, South 1, West 16, Chuo-ku, Sapporo 060-8543, Japan*
[2] *Otaru Dermatology Clinic, Otaru 047-0032, Japan*

Correspondence should be addressed to Akihiro Yoneta, yonetaa@sapmed.ac.jp

Basal cell carcinoma (BCC) is the most common skin tumor and contains several different histopathological types. Here, we report a case of cystic basal cell carcinoma, which is relatively rare and might be clinically misdiagnosed. A dermatoscopic examination of the case revealed a homogenous blue/black area usually not seen in BCC. We reviewed 102 BCC cases resected and diagnosed at Sapporo Medical University Hospital between April 2005 and March 2010. Among them, only three were the cystic type.

## 1. Case Report

An 80-year-old woman with a nodular lesion on her right breast was referred to our outpatient clinic in January 2010 after she had visited a local dermatology clinic. According to the patient, the lesion had existed since her early childhood, and its size had gradually been increasing. Clinical differential diagnosis included pigmented nevus and adnexal tumors as well as BCC.

A dermatological examination revealed a well-demarcated blue/black colored nodule, measuring 10 × 7.0 cm in size, on her right breast (Figure 1). A dermatoscopic examination showed a homogenous blue/black area in the center of the lesion with arborizing telangiectasia in the periphery to the surrounding region (Figure 2).

The tumor was excised with a tumor free margin of 1 cm. Histopathological findings showed tumor masses mostly on the dermis with continuation from the epidermis in some parts. The tumor contained cystic spaces as well as palisading of the basaloid cells at the peripheral sites of the tumor masses and clefts between the stroma and tumor edge, which are often seen in typical basal cell carcinomas (Figure 3).

## 2. Discussion

Basal cell carcinoma is a slowly growing malignant epithelial skin tumor predominantly affecting middle-aged and fair-skinned individuals [1]. Histopathologically, BCCs are composed of islands or nests of basaloid cells, with palisading of the cells at the periphery and a haphazard arrangement of those in the centers of the islands. Various morphological subtypes have been defined. These include solid, micronodular, cystic, multifocal superficial, pigmented, adenoid, infiltrating, sclerosing, keratotic, infundibulocystic, metatypical, basosquamous, and fibroepitheliomatous [2]. Histological differential diagnosis should include trichoblastoma. Criteria that may have value in distinguishing trichoblastomas from BCC include the following: the presence in the former of symmetry, circumscription with smooth margins and "shelling out" of the normal tissue, follicular and "racemiform" patterns of lesional cells, or the lack of a clefting artifact between stroma and epithelium that is characteristic of BCC [3]. In the present case, the tumor masses are relatively asymmetrically distributed, and clefts between the stroma and tumor edge are observed.
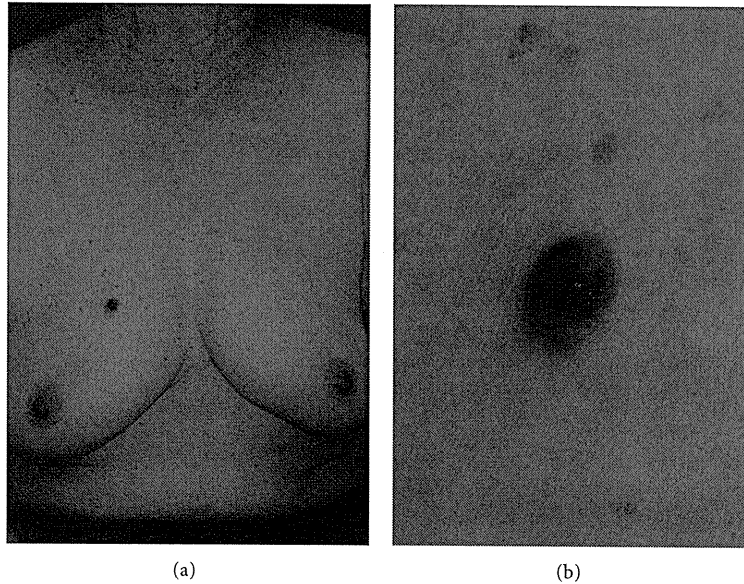
(a)                                           (b)

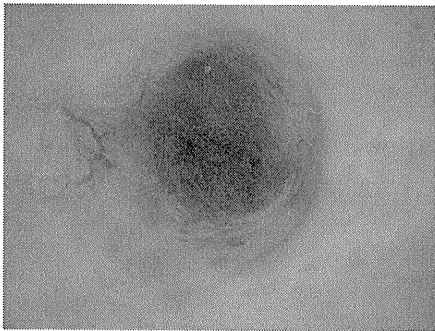FIGURE 1: (a) A well-demarcated blue/black nodule was recognized on the right anterior chest. (b) high maginification.



FIGURE 2: Dermatoscopic examination showed a homogenous blue/black area and arborizing telangiectasia.

TABLE 1: Histopathological types of BCC cases at Sapporo Medical University between April 2005 and March 2010.

| Histopathological types | Number of cases (%) | |
| --- | --- | --- |
| Solid | 56 | (54.9) |
| Multifocal superficial | 10 | (9.8) |
| Micronodular | 8 | (7.8) |
| Sclerosing | 8 | (7.8) |
| Adenoid | 6 | (5.9) |
| Infiltrating | 5 | (4.9) |
| Cystic | 3 | (2.9) |
| Fibroepitheliomatous | 3 | (2.9) |
| Keratotic | 1 | (1.0) |
| Infundibulocystic | 1 | (1.0) |
| Basosquamous | 1 | (1.0) |
| Total | 102 | (100) |

Noninvasive procedures have been developed for the diagnosis of skin cancers [4–7]. Among these, dermatoscopy is the most useful diagnostic procedure with the highest clinical impact in dermatologic practice to better differentiate benign from malignant skin lesions and to detect tumors in the early stage [6, 7].

The model for the diagnosis of the pigmented variant of BCC is based on the absence of a pigmented network to differentiate it from melanoma and the presence of at least one positive feature including (1) ulceration (not associated with a recent history of trauma), (2) multiple blue/gray globules, (3) leaf-like areas, (4) large blue/gray ovoid nests, (5) spoke-wheel areas, and (6) arborizing telangiectasia [8]. However, BCC may exhibit a large variety of clinical and dermatoscopic characteristics because of its wide range of histopathological features [9].

In the present case, the pigment network was absent and, among the six features, arborizing telangiectasia was present but the other features were not. Instead, a homogenous blue/black area was seen in the center of the tumor, which could be distinguished from the large blue/gray ovoid nests. Histologically, cystic areas overlay the tumor, which may have been the reason for the homogenous blue/black area. The mechanism of the cyst formation was assumed to be massive cell necrosis in the central part of the tumor, which was caused by the rapid tumor growth [1].

We evaluated 102 cases of BCC diagnosed at our hospital between April 2005 and March 2010. They were classified into pathological subtypes as shown in Table 1. The solid type was the most frequent in our database as reported elsewhere [2]. The cystic type was relatively rare (2.9%) in the present study (Table 1). Among two other cases of the cystic type, in one, the patient did not undergo a dermatoscopic

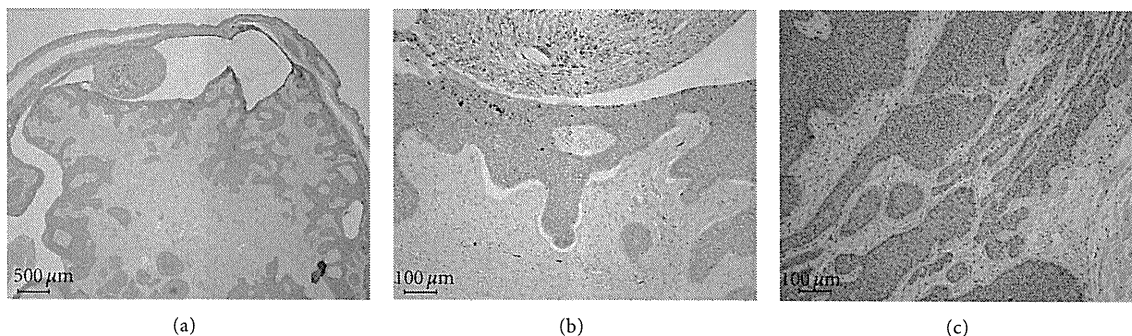(a)                                    (b)                                    (c)

FIGURE 3: (a) Histological finding showed tumor masses mostly on the dermis with continuation from the epidermis in some parts. The tumor contains cystic spaces. (b) Clefts between the stroma and tumor edge are seen. (c) Palisading of the basaloid cells at the peripheral sites of the tumor masses is noticed.
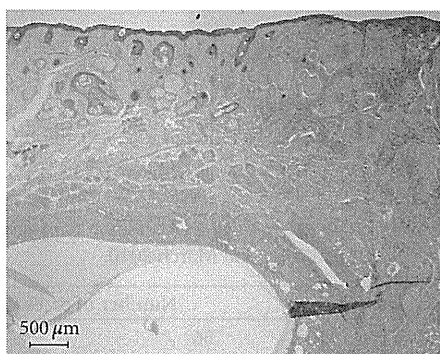


FIGURE 4: Histological examination showed multiple variably sized nodules with continuation of the epidermis. A cystic area underlies the tumor masses.
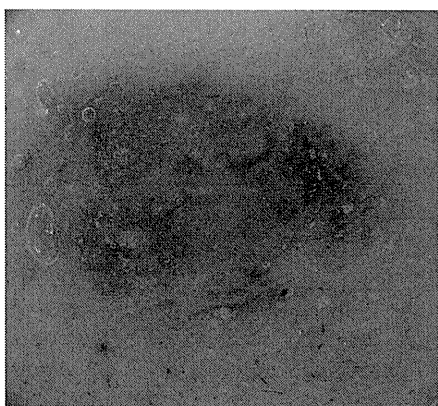


FIGURE 5: Dermatoscopic examination showed multiple blue/gray globules and arborizing telangiectasia, lacking a homogenous blue/black area.

examination. In the other case, multiple blue/gray globules and arborizing telangiectasia were observed, but there were no homogenous blue/black areas (Figure 4). This may be due to the fact that, unlike the present case, a cystic area existed under tumor masses (Figure 5).

## 3. Conclusions

In conclusion, we herein reported a cystic BCC showing a blue/black nodule on the right chest wall. Dermatoscopy revealed a homogenous blue/black area with arborizing telangiectasia. This rare clinical appearance made it difficult to diagnose; however, our findings suggest that BCC should be considered when a dermatoscopic examination reveals a cystic lesion with a homogenous blue/black area with arborizing telangiectasia.

## Abbreviations

BCC: basal cell carcinoma.

## References

[1] D. Altamura, S. W. Menzies, G. Argenziano et al., "Dermatoscopy of basal cell carcinoma: morphologic variability of global and local features and accuracy of diagnosis," *Journal of the American Academy of Dermatology*, vol. 62, pp. 67–75, 2010.

[2] D. Weedon, *Skin Pathology*, Churchhill Livingstone, Edinburgh, UK, 2nd edition, 2002.

[3] D. E. Elder, *Lever's Histopathology of the Skin*, Lippincott Williams & Wilkins, Philadelphia, Pa, USA, 9th edition, 2005.

[4] H. Kittler, H. Pehamberger, K. Wolff, and M. Binder, "Diagnostic accuracy of dermoscopy," *Lancet Oncology*, vol. 3, no. 3, pp. 159–165, 2002.

[5] A. A. Marghoob, L. D. Swindle, C. Z. M. Moricz et al., "Instruments and new technologies for the in vivo diagnosis of melanoma," *Journal of the American Academy of Dermatology*, vol. 49, no. 5, pp. 777–797, 2003.

[6] S. W. Menzies, K. Westerhoff, H. Rabinovitz, A. W. Kopf, W. H. McCarthy, and B. Katz, "Surface microscopy of pigmented basal cell carcinoma," *Archives of Dermatology*, vol. 136, no. 8, pp. 1012–1016, 2000.

[7] M. Mogensen and G. B. E. Jemec, "Diagnosis of nonmelanoma skin cancer/keratinocyte carcinoma: a review of diagnostic accuracy of nonmelanoma skin cancer diagnostic tests and technologies," *Dermatologic Surgery*, vol. 33, no. 10, pp. 1158–1174, 2007.

[8] J. Roewert-Huber, B. Lange-Asschenfeldt, E. Stockfleth, and H. Kerl, "Epidemiology and aetiology of basal cell carcinoma,"

*British Journal of Dermatology*, vol. 157, supplement 2, pp. 47–51, 2007.

[9] M. Ulrich, E. Stockfleth, J. Roewert-Huber, and S. Astner, "Noninvasive diagnostic tools for nonmelanoma skin cancer," *British Journal of Dermatology*, vol. 157, supplement 2, pp. 56–58, 2007.

## ORIGINAL ARTICLE

# Rab7 is a critical mediator in vesicular transport of tyrosinase-related protein 1 in melanocytes

Tokimasa HIDA,[1,2] Hitoshi SOHMA,[2] Yasuo KOKAI,[3] Akinori KAWAKAMI,[1] Kuninori HIROSAKI,[1] Masae OKURA,[1] Noriko TOSA,[4] Toshiharu YAMASHITA,[1] Kowichi JIMBOW[1,5]

[1]Department of Dermatology, Sapporo Medical University School of Medicine, [2]Department of Educational Development, Sapporo Medical University Center for Medical Education, [3]Department of Biomedical Engineering, Sapporo Medical University School of Medicine, [4]Institute for Animal Experimentation, Hokkaido University Graduate School of Medicine, and [5]Institute of Dermatology and Cutaneous Sciences, Sapporo, Japan

## ABSTRACT

How melanosomal proteins such as enzymic proteins (tyrosinase and tyrosinase-related proteins, Tyrps) and structural protein (gp100) are transported from Golgi to melanosomal compartments is not yet fully understood. A number of small GTPases have been found to be associated with melanosomes and we have identified one of them, Rab7, a regulator of vesicular transport, organelle motility, phospholipid signaling and cytosolic degradative machinery, as being involved in the transport of Tyrp1 from Golgi to stage I melanosomes. This study further characterizes the role of Rab7 as a regulator of differential sorting of melanosomal proteins in this process. Murine melanocytes were transiently transfected with a plasmid encoding either wild-type (Rab7WT), constitutively active (Rab7Q67L) or dominant-negative (Rab7N125I and Rab7T22N) Rab7. Through immunocytostaining and confocal laser scanning microscopy, we quantitatively compared the bio-distribution of melanosomal proteins between Rab7WT-expressing cells and mutant Rab7-expressing cells. We also characterized their differential elimination from melanosomal compartments by Rab7 by utilizing a proteasome inhibitor, MG132. Our findings indicate that Rab7 plays an important role in differential sorting of tyrosinase, Tyrp1 and gp100 in early melanogenesis cascade, and that it is more specifically involved with Tyrp1 than tyrosinase and gp100 in the trafficking from Golgi to melanosomes and the specific exit from the degradative process.

Key words: gp100, melanogenesis, melanosome, tyrosinase, tyrosinase-related protein, Tyrp1.

## INTRODUCTION

Melanosomes are melanocyte-specific organelles that produce and store melanin pigments inside. They are lysosome-related organelles, sharing several important properties common to lysosomes, such as the presence of luminal and membrane lysosomal proteins, an acidic luminal environment, accessibility to endocytic tracers and the ability to fuse with phagosomes.[1] They undergo four maturation stages with distinctive morphological changes.[2,3] Once they

fully mature, they are stored in the peripheral area or in the cell processes and are transferred to adjacent keratinocytes.

Tyrosinase and its related proteins (tyrosinase-related proteins 1 and 2, Tyrp1 and 2) are the membrane glycoproteins and major melanosomal enzymes. Tyrosinase is a key enzyme that catalyzes the oxidation of tyrosine to dopaquinone which is a source for both black/brown eumelanin and red/yellow pheomelanin.[4,5] Tyrp1 has dihydroxyindole carboxylic acid oxidase activity while Tyrp2 has

dopachrome tautomerase activity, and both are related to the eumelanin synthesis.[4,6] Tyrp1 is also associated with tyrosinase in melanosomes and functions as a tyrosinase-stabilizer.[7] The loss or dysfunction of tyrosinase and Tyrp1 results in oculocutaneous albinism types 1 and 3, respectively.[8,9] gp100 (also known as Pmel17) is another unique melanosomal glycoprotein that is synthesized as a type 1 integral membrane protein and is cleaved off enzymatically in post-Golgi compartments.[10] The cleaved fragments accumulate in the lumina of stage I/II melanosomes and form unique striated structures on which newly-synthesized melanin is deposited.[3] gp100-associated albinism has not been reported in humans, but dysfunction of gp100 in mice causes premature death of follicular melanocytes, resulting in a unique hair color pattern (*silver* phenotype). Not only the dysfunction of these melanosomal proteins but also their transport failure, results in depigmentation disorders such as Hermansky–Pudlak syndrome.[11]

Both tyrosinase and Tyrp1 are transported from the *trans*-Golgi network to melanosomes through endosomal compartments. Adaptor proteins (AP) generate transport vesicles, sort proteins and assemble clathrin in the post-Golgi network.[12] AP-3 binds to a dileucine motif of tyrosinase.[13–15] Tyrosinase can use both AP-1 and AP-3 for its proper sorting while Tyrp1 can use only AP-1.[2,14,16] This suggests that they use different transport pathways even though they have similar protein structures and functional domains, including the dileucine motif.

Rab7 is a member of the Rab small glutamyl transpeptidase (GTP)-binding protein family and, by affecting its effector molecules, is essential for the regulation of vesicular transport, organelle motility, phospholipid signaling, phagocytosis and autophagocytosis.[17–29] Our previous study of charactering the fractionated melanosome-associated proteins found that Rab7 was associated with the melanosomal membrane of B16 murine melanoma cells and was involved in the transport of Tyrp1.[30] We also reported that exogenously-expressed Tyrp1 was localized to early endosomes in human amelanotic melanoma cells when Rab7 was inhibited.[31] These findings suggest that the transport of Tyrp1 requires functional Rab7 and that Tyrp1 passes through endosomal compartments. However, it is still not clarified whether

Rab7 is involved in the transport of other major melanosomal proteins such as tyrosinase and gp100, and if it is, to what extent. It also remains uncertain whether Rab7 functions in the trafficking of melanosomal proteins in non-tumorigenic melanocytes. Here, we transfected immortal melanocytes with plasmids carrying cDNA of wild-type and mutant Rab7, and analyzed their differential effects on the intracellular trafficking of endogenous tyrosinase, Tyrp1 and gp100 by single-cell observation with immunofluorescent staining and confocal laser scanning microscopy. We found that the inhibition of Rab7 led to preferential Tyrp1 elimination from melanocytes. Our results indicate that the transport pathway of Tyrp1 to melanosomes is different from that of tyrosinase and gp100 and that Rab7 is a crucial regulator for Tyrp1 sorting in the endosomal compartment, promoting its exit from the degradative process.

## METHODS

### Vector construction
*Rab7WT*, a cDNA of wild-type Rab7, was amplified from pGEM-canine Rab7[32] by using the N-terminal flag sequence-containing primer with the *Hind*III site and C-terminal primer with the same restriction site. Oligonucleotides used for the amplification were 5′-CCC <u>AAG CTT</u> ACC ATG *GAC TAC AAG GAT GAC GAT GAC AAG* ACC TCT AGG AAG AAA GTG TTG-3′ and 5′-CCC <u>AAG CTT</u> TCA GCA ACT GCA GCT TTC CGC-3′ (underlines indicate the *Hind*III site, and italics the flag sequence). A cDNA of Rab7N125I was constructed through polymerase chain reaction-mediated mutagenesis[33] by which a partial sequence of the flag-tagged *Rab7WT* oligonucleotide was modified as A374T for *Rab7N125I*. The fragment of flag-tagged *Rab7N125I* was inserted into the *Hind*III site of pcDNA3.1/Hygro (+) (Invitrogen, Carlsbad, CA, USA). The inserted cDNA was verified by nucleotide sequencing. p3xFLAG-CMV-7.1 fused with cDNA of *Rab7T22N* or *Rab7Q67L* was described previously.[34]

### Cell culture and transient transfection
Melan-A cells, kindly provided by Dr Dorothy C. Bennett, UK, were cultured on coverslips in RPMI-1640 medium (Sigma-Aldrich, St Louis, MO, USA) supplemented with 10% fetal bovine serum, 200 nmol/L phorbol myristate acetate, 100 U/mL penicillin and

100 mg/L streptomycin sulfate in a 10% $CO_2$ atmosphere. Transfection was performed by using FuGENE6 (Roche Diagnostics, Basel, Switzerland) according to the manufacturer's protocol. Cells grown on round coverslips coated with 1% porcine skin gelatin (Sigma-Aldrich) were transfected with 0.5 μg of plasmid DNA and cultured for 24 or 48 h according to the examination. When proteasome inhibitor was necessary, cells were incubated with 10 μmol/L MG132 (Sigma-Aldrich) for 5 h prior to the fixation.

### Immunofluorescent staining and confocal laser scanning microscopy

Anti-PEP7, a rabbit polyclonal antiserum against tyrosinase, was kindly provided by Dr Vincent J. Hearing, USA. HMSA5, a mouse monoclonal antibody against Tyrp1, was developed previously.[35] HMB45, a mouse monoclonal antibody against gp100 was purchased from DAKO (Glostruk, Denmark). An anti-flag mouse monoclonal antibody (clone M2) and a rabbit anti-flag polyclonal antibody were purchased from Sigma. Goat antimouse and antirabbit immuno-globulin G antibodies conjugated with Alexa Fluor 488 or Alexa Fluor 594 were products of Invitrogen. Immunofluorescent staining was performed as described previously with a slight modification.[31] Cells were fixed in a mixture of acetone and methanol (1:1) at −20°C for 5 min. After a brief wash with phosphate buffered saline containing 0.5% (w/v) bovine serum albumin, a pair of monoclonal and polyclonal primary antibodies was used simultaneously for double staining. The antibody dilution was as follows: HMSA5, 1:1000; anti-flag M2, 1:1000; and polyclonal anti-flag, 1:2000. The secondary fluorescent-labeled antibodies were used at a dilution of 1:600. The coverslips were mounted with Permafluor (Beckmann Coulter Immunotech, Marseille, France) on glass slides. Immunofluorescent images were obtained by confocal laser scanning microscopy using an Axiovert 100M (Carl Zeiss, Thornwood, NY, USA) equipped with LSM510 V2.5 (Carl Zeiss). Transfected and un-transfected cells were simultaneously included in every recorded image.

### Fluorometric analysis and statistics

Confocal images were collected and fluorometric analysis was carried out with ImageJ 1.36b (National Institute of Health, Bethesda, MD, USA). From each confocal image, the relative fluorescence in trans-fected cells to that in untransfected cells was calculated and categorized into four groups depending on the value: 0–0.1, 0.1–0.5, 0.5–2 and more than 2. The proportion of each group was statistically analyzed using Pearson's $\chi^2$-test (5% significance level).

## RESULTS

### Subcellular localization of wild-type and mutant Rab7

To observe the effect of Rab7 mutants directly and to compare the distribution of Tyrp1 in transfected and untransfected cells, the plasmids carrying wild-type *Rab7* (*Rab7WT*), a constitutively active mutant (*RabQ67L*) and dominant-negative mutants (*Rab7N-125I* and *Rab7T22N*) were transfected to Melan-A melanocytes. The addition of the tag sequences to Rab proteins does not appear to alter their function or subcellular localization.[17] Twenty-four hours after the transfection, the cells were doubly immunostained with the anti-flag antibody and anti-Tyrp1 antibody. Rab7WT distributed on fine granules mostly in the perinuclear area (Fig. 1a). The granules were not well-demarcated, which suggested that Rab7WT existed as membrane-free molecules as well as mem-brane-bound ones. Tyrp1 was partly co-localized with the Rab7WT-positive granules in the perinuclear area (Fig. 1a, inset), but most Tyrp1-positive granules in the peripheral area or in dendrites were Rab7 negative. In Rab7Q67L-expressing cells, Tyrp1 was localized in perinuclear, enlarged granules and co-localized with Rab7Q67L (Fig. 1b). In the cells expressing Rab7N125I (Fig. 1c) or Rab7T22N (Fig. 1d), mutant Rab7 were distributed throughout the cytoplasm with-out showing localization to a particular organelle, though Rab7N125I was also detected in conglomer-ated structures in the juxtanuclear area. Because these structures did not show any co-localization with early or late endosomal markers, or with a Golgi mar-ker (data not shown), we concluded that they were excess Rab7N125I molecules and were being degraded. Interestingly, only a small number of Tyrp1-positive granules were detected in the perinuclear area in the cells expressing Rab7N125I or Rab7T22N (Fig. 1c,d).
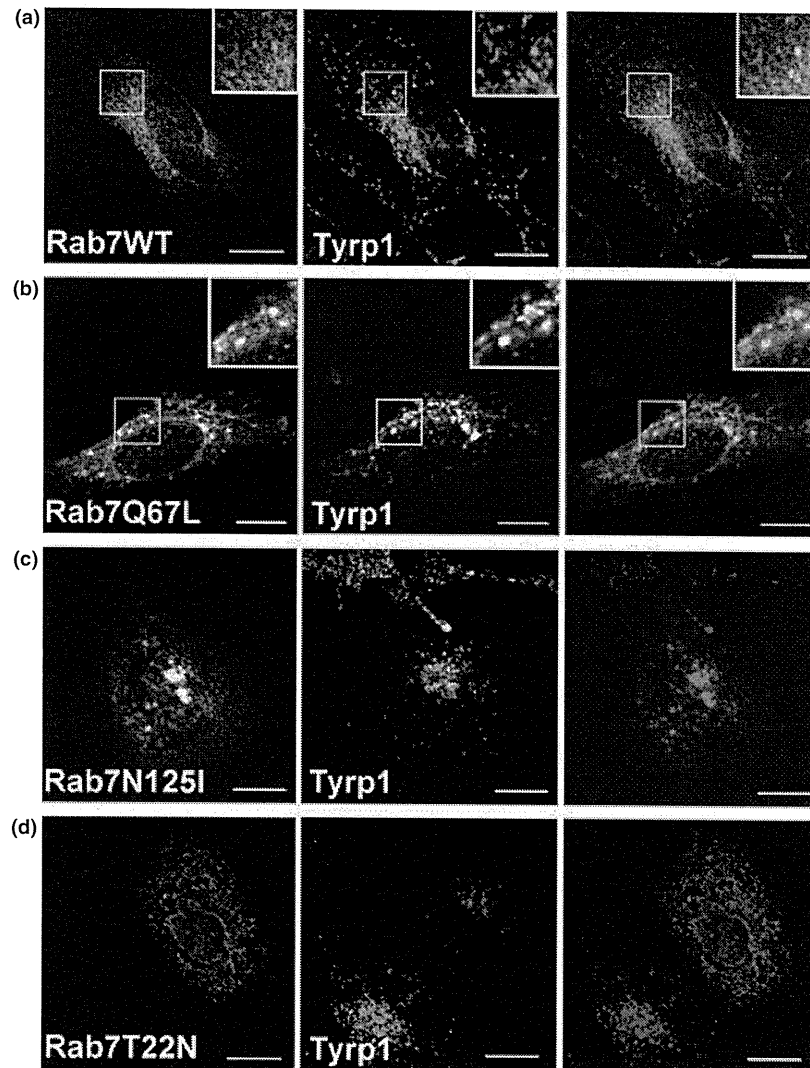
**Figure 1.** Tyrp1 was less prominent in the cells expressing dominant negative Rab7 24 h after the transfection. Melan-A cells were transfected with the plasmids encoding Rab7WT (a), Rab7Q67L (b), Rab7N125I (c) and Rab7T22N (d). Twenty-four hours later, they were immunostained with the anti-flag antibody (a–d, left) and anti-Tyrp1 antibody (a–d, middle). Merged images are shown on the right. Scale bars = 10 μm.

## Tyrp1 was gradually eliminated from dominant-negative Rab7 expressing cells

To investigate if the reduced Tyrp1 immunostaining in the cells expressing mutant Rab7 reflected the static state of Tyrp1 localization, we observed transfected cells at two time points: 24 h and 48 h after the transfection. In Rab7WT-expressing cells, the amount and distribution of Tyrp1-positive granules were comparable with those in surrounding non-transfected cells at both time points (Fig. 2a,b). In contrast,

Rab7N125I-expressing cells showed reduced Tyrp1 immunostaining in the perinuclear area at 24 h (Fig. 2c) and, surprisingly, no Tyrp1 immunostaining was detected in the cells at 48 h (Fig. 2d). The Tyrp1 elimination at the later time point after the transfection was also observed in Rab7T22N-expressing cells (data not shown).

To verify this phenomenon, 30 transfected melanocytes were randomly selected from each sample and were categorized into four groups according to their
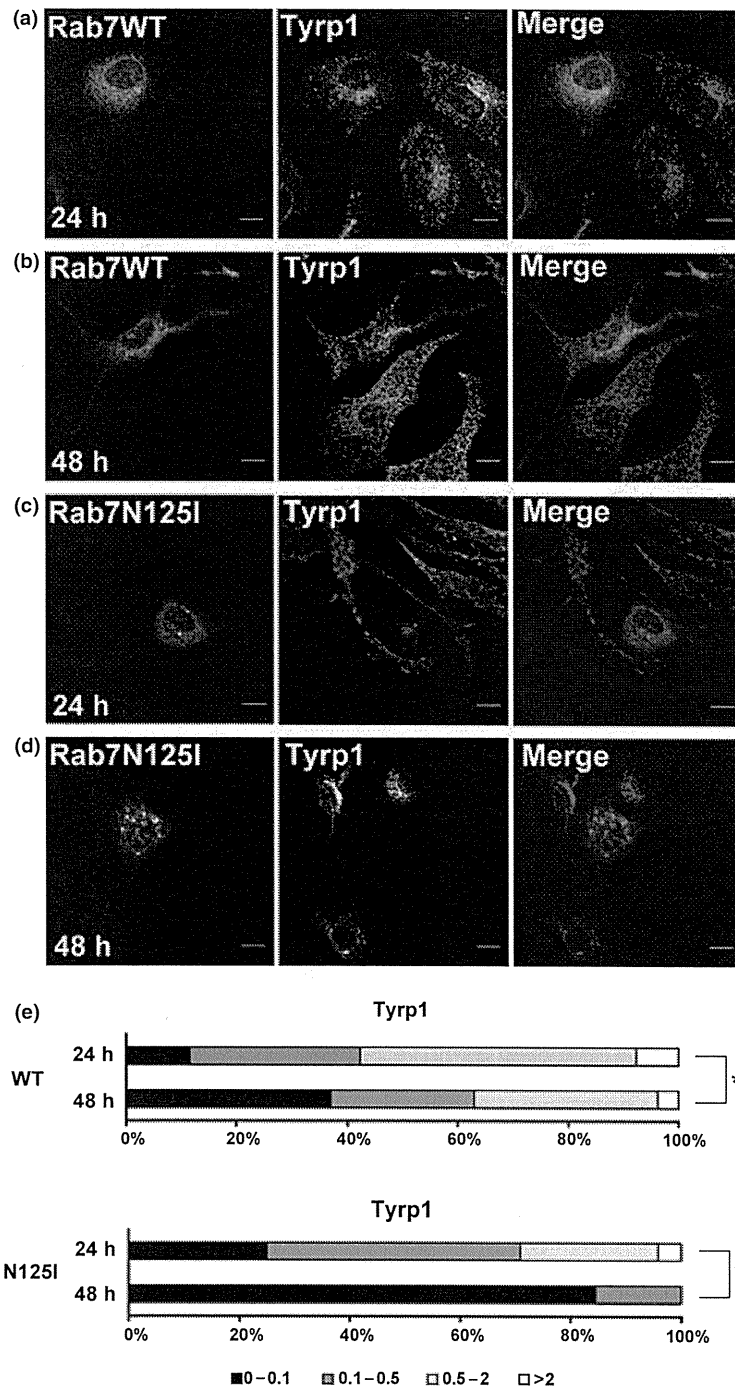
**Figure 2.** Tyrp1-positive granules were eliminated 48 h after the transfection of Rab7N125I. Melan-A cells were transfected with the plasmids encoding Rab7WT (a,b) or Rab7N125I (c,d), and incubated for 24 h (a,c) or 48 h (b,d) before fixation. Cells were immunostained with the anti-flag antibody (a–d, left) and anti-Tyrp1 antibody (a–d, middle). Merged images are shown on the right. Scale bars = 10 μm. (e) Tyrp1-elimination was statistically verified. Thirty cells expressing Rab7WT or Rab7N125I for 24 h and the same number of the cells expressing it for 48 h were categorized into four types according to the relative intensity of Tyrp1 immunostaining to that in surrounding control cells: 0–0.1, 0.1–0.5, 0.5–2 and >2. Bars show the percentage of each cell pattern. *$P$ = 0.18. †$P$ = 0.00023. WT, Rab7WT-expressing cells; N125I, Rab7N125I-expressing cells.

Tyrp1-signal intensities relative to that of surrounding control cells: 0–0.1, 0.1–0.5, 0.5–2.0 and more than 2 (Fig. 2e). In Rab7WT-expressing cells, the proportion of the groups at 24 h and 48 h were not significantly different ($P$ = 0.181). On the other hand, in Rab7N125I-expressing cells, it was quite different at 48 h ($P$ = 0.00023) when the relative Tyrp1 intensity was less than 0.1 in 85% of the cells. These results suggested that the reduction or elimination of Tyrp1 occurred in the vast majority of the Rab7N125I-expressing cells.

## Rab7N125I specifically eliminated Tyrp1, but not tyrosinase or gp100

We further investigated if inhibition of Rab7 led to elimination of other major melanosomal proteins. The distribution of Tyrp1, tyrosinase and gp100 was examined 48 h after the transfection of Rab7WT or Rab7N125I. Tyrp1-positive granules in Rab7WT-expressing and untransfected cells were similarly distributed in the perinuclear and peripheral areas (Fig. 3a). Tyrp1 was not detected in the Rab7N125I-expressing cells. Tyrosinase-positive granules in Rab7WT-expressing cells, as well as control cells, were also distributed similarly (Fig. 3b). Unlike Tyrp1, tyrosinase-positive granules were observed in the Rab7N125I-expressing cells. In Rab7WT-expressing cells and control cells, gp100-positive granules were distributed in both the perinuclear and peripheral areas (Fig. 3c). The amount of gp100-positive granules in Rab7N125I-expressing cells was comparable to those in control cells. Interestingly, gp100-positive granules in the Rab7N125I-expressing cells were distributed mainly in the peripheral area. These results suggested that inhibition of Rab7 led to elimination of Tyrp1 but did not affect tyrosinase or gp100.

To support these results, the immunostaining results were statistically analyzed (Fig. 3d). Approximately 68 digital images (ranging 55–75 images) of the cells expressing Rab7WT or Rab7N125I were categorized into four groups as described in the previous paragraph. The intensity of Tyrp1 immunostaining in Rab7N125I-expressing cells was clearly different from that of Rab7WT-expressing cells ($P$ < 0.00001). In 84% of Rab7N125I-expressing cells, the intensity was less than 0.1. In contrast, the difference in the intensity between Rab7WT- and Rab7N125I-

expressing cells was not statistically significant in the cases of tyrosinase and gp100 ($P$ = 0.291 and 0.729, respectively).

## Proteasome inhibitor partially rescued the Tyrp1 elimination by Rab7 mutants

We hypothesized that Tyrp1 failed to be sorted properly in endosomal compartments, was mislocalized to lysosomes and then quickly degraded under the inhibition of Rab7. Proteasomal activities are necessary for some membrane proteins to translocate from the limited membrane to inner vesicles of multivesicular bodies.[36–38] We examined if Tyrp1 elimination could be rescued by proteasomal inhibitor MG132. Melan-A cells were transfected with the plasmid encoding Rab7N125I or Rab7T22N and incubated for 43 h with growth medium, followed by 5 h incubation with the medium containing MG132. Tyrp1-positive granules were detected in the perinuclear areas of the cells incubated with MG132 whereas they were not in the cells without MG132 (Fig. 4a–d).

To confirm the results, 30 cells incubated with MG132 and the same number of cells incubated without MG132 were randomly selected, and categorized into four groups as described in the previous paragraph (Fig. 4e). Nearly 90% of the mutant Rab7-expressing cells (either Rab7N125I or Rab7T22N) showed low relative signal intensity (0–0.1). In contrast, when the cells were treated with MG132, cells with the relative signal intensity of more than 0.1 clearly increased. Furthermore, 20% and 33% of the cells expressing Rab7N125I and Rab7T22N, respectively, showed amounts of Tyrp1 comparable to control cells (relative intensity of 0.5–2).

To exclude the possibility that the increase of Tyrp1 was simply caused by MG132 regardless of mutant Rab7 expression, Melan-A cells without mutant Rab7 expression were incubated as described above and immunostained with the anti-Tyrp1 antibody. Tyrp1-positive granules were similarly distributed in both MG132-treated and -untreated cells: concentrated in the perinuclear area and scattered in the cytoplasm (Fig. 4f). Fluorescent intensity of Tyrp1 in MG132-treated cells was comparable to that in MG132-untreated cells (Fig. 4g). These results suggest that Tyrp1 elimination in the cells expressing mutant Rab7 was partially rescued by the proteasomal inhibitor.